MycoKeys 129: 81 –105 (2026)
DOI: 10.3897/mycokeys.129.182847

Research Article

Three new species of *Gnomoniopsis* and *Ternstroemiomyces* (Diaporthales, Sordariomycetes) from China

Zheng-Hu Guo[1*], Ya-Qin Zhou[2*], Jie Wang[1], Li-Ying Yu[2], Shou-Jie Qin[1], Jia-Xin Liu[1], Yu Chen[1], Rong-Shao Huang[1,3], Xiao-Ming Tan[1,3,4]

1 *College of Pharmacy, Guangxi University of Chinese Medicine, Nanning 530200, China*
2 *Guangxi Botanical Garden of Medicinal Plant, Nanning 530023, China*
3 *Engineering Research Center for High-value Utilization of Guangxi-specific Genuine Medicinal Materials, Nanning 530200, China*
4 *Guangxi Key Laboratory of Zhuang and Yao Ethnic Medicine, Guangxi University of Chinese Medicine, Nanning 530200, China*
Corresponding author: Xiao-Ming Tan (tanxm@gxtcmu.edu.cn)

Abstract

Cinnamomum cassia is a renowned medicinal and aromatic plant with significant economic importance and broad pharmacological applications. This study investigates the taxonomy and diversity of endophytic fungi belonging to the order Diaporthales, isolated from this plant in Guangdong Province, China. A total of six isolates were obtained from healthy leaves. These isolates were examined using morphological characteristics and multilocus phylogenetic analyses based on the internal transcribed spacer (ITS), large subunit ribosomal RNA gene (LSU), and translation elongation factor 1-alpha (*tef1*). Phylogenetic reconstructions inferred from maximum likelihood and Bayesian inference, together with morphological evidence, revealed that the isolates represent three distinct and previously undescribed species, which are herein described as *Gnomoniopsis luodingensis* **sp. nov.** (Gnomoniaceae), *Ternstroemiomyces cinnamomi* **sp. nov.**, and *Ternstroemiomyces zhaoqingensis* **sp. nov.** (Ternstroemiomycetaceae). These findings expand the known host range of endophytic fungi and provide essential taxonomic data for the fungal community associated with this economically important medicinal plant.

Key words: Endophytic fungi, morphology, phylogenetic analysis

OPEN ACCESS

Academic editor:
Nalin Wijayawardene
Received: 18 December 2025
Accepted: 9 February 2026
Published: 23 February 2026

Citation: Guo Z-H, Zhou Y-Q, Wang J, Yu L-Y, Qin S-J, Liu J-X, Chen Y, Huang R-S, Tan X-M (2026) Three new species of *Gnomoniopsis* and *Ternstroemiomyces* (Diaporthales, Sordariomycetes) from China. MycoKeys 129: 81–105. https://doi.org/10.3897/mycokeys.129.182847

Copyright: © Zheng-Hu Guo et al.
This is an open access article distributed under terms of the Creative Commons Attribution License (Attribution 4.0 International – CC BY 4.0).

Introduction

The Diaporthales (Sordariomycetes, Ascomycota) comprises a widespread fungal group with substantial ecological and economic importance (Senanayake et al. 2017). This order includes well-known phytopathogens such as *Cryphonectria parasitica*, the causal agent of chestnut blight, as well as numerous species of *Diaporthe* that are associated with diseases in a wide range of crops (Miller and Lewis Ivey 2025; Zhao et al. 2025). In addition to their roles as pathogens, members of Diaporthales function as saprobes or as endophytes on the various plants in recent years (Gomes et al. 2013; Bai et al. 2023; Li et al. 2025a). Endophytic species colonize healthy plant tissues without inducing

* These authors contributed equally to this work.

visible symptoms and can contribute to plant growth promotion and enhanced resistance (Sun et al. 2019; Pereira et al. 2023). They are also known to produce biologically active secondary metabolites, demonstrating considerable potential for applications in medicine and agriculture (Saravanakumar et al. 2021; Xu et al. 2021; Jiang et al. 2023). Currently, Diaporthales is considered to include 35 families supported by combined morphology and molecular phylogeny (Zhang et al. 2025).

Gnomoniaceae is a distinct family of Diaporthales, and was first established by Winter (1886). This family was circumscribed by Sogonov et al. (2008), and this taxonomic concept has been followed by others. *Gnomoniopsis* Berl. (Gnomoniaceae) was initially described as a subgenus within *Gnomonia* Ces. & De Not. because of their similar morphology. However, *Gnomoniopsis* has been separated from *Gnomonia* by means of morphology, phylogeny and host associations (Sogonov et al. 2008; Walker et al. 2010). Species of *Gnomoniopsis* occur as endophytes, saprobes, or pathogens, with some exhibiting a latent pathogenic lifestyle (e.g., *G. castaneae*) (Dobry and Campbell 2023). They predominantly inhabit families such as Rosaceae, Fagaceae, and Onagraceae. Consequently, investigating their diversity in asymptomatic tissues is vital for understanding their ecological potential and pathogenicity. According to Index Fungorum (http://www.indexfungorum.org/, accessed on 20 Nov. 2025), approximately 50 names have been recorded for *Gnomoniopsis*.

The family Ternstroemiomycetaceae, currently comprising a single genus *Ternstroemiomyces* with two species (*Te. ternstroemiae* and *Te. machili*), was established based on a leaf-inhabiting fungus isolated from *Machilus nanmu* (Oliv.) Hemsl. and *Ternstroemia gymnanthera* (Wight & Arn.) Bedd. Ternstroemiomycetaceae is closely associated with Erythrogloeaceae, forming a distinct clade within a larger branch, yet showing clear divergence. The family is characterized by its pycnidial conidiomata that exude slimy, orange conidial masses, and produces hyaline, multi-guttulate conidia (Zhang et al. 2025). Due to its recent establishment and limited number of known species, the diversity and host range of Ternstroemiomycetaceae remain poorly understood.

Cinnamomum cassia (Lauraceae) is an economically important tree species cultivated for its dried bark, a popular spice and traditional medicinal herb with broad market demand (Cheng et al. 2024). Its pharmacological components have antioxidant, antibacterial and anti-inflammatory effects (Zhang et al. 2019). To date, research on *C. cassia* has largely focused on its volatile oil composition and pharmacological activities (Zhang et al. 2019), while the diversity of its endophytic fungi remains underexplored (Lv et al. 2024). A comprehensive assessment of endophytic fungal diversity in *C. cassia* is fundamental to evaluating potential disease risks, exploring beneficial microbial resources, and improving our understanding of plant–microbe interactions.

In this study, several Diaporthales isolates were obtained during a survey of endophytic fungal diversity in *C. cassia*. Through integrated morphological observations and multilocus phylogenetic analyses based on the internal transcribed spacer (ITS), the large subunit ribosomal RNA gene (LSU), and the translation elongation factor 1-alpha gene (*tef1*), we identified three new species: *Gnomoniopsis luodingensis* sp. nov. (Gnomoniaceae), *Ternstroemiomyces cinnamomi* sp. nov., and *Ternstroemiomyces zhaoqingensis* sp. nov. (Ternstroemiomycetaceae). This study contributes to the known species diversity of

Diaporthales and provides new insights into the ecological role of *C. cassia* as a fungal host. Furthermore, it establishes an essential taxonomic basis for future research into the biology and host interactions of these novel species.

Materials and methods

Sample collection and fungal strain isolation

In October–November 2022, the healthy leaves of *Cinnamomum cassia* were collected in Zhaoqing and Luoding, Guangdong Province, and brought to the laboratory on the same day. The leaf samples were stored at 4 °C, and all isolation procedures were completed within 24 h. The procedures used for the surface sterilization of the samples were according to the methods described by Zhou et al. (2022). The samples were sequentially surface-sterilized in 75% ethanol for 30 s, in 2.5% sodium hypochlorite for 4–5 min, and then rinsed three times in sterile distilled water for 30 s. Subsequently, the leaves were cut into 0.5 cm × 0.5 cm pieces using a sterile scalpel. A total of 225 tissue segments were transferred to potato dextrose agar (PDA; containing 200 g/L potato, 20 g/L glucose, and 20 g/L agar) and cultured at 25 °C. Finally, 93 endophytic fungal strains were isolated from these tissue segments.

Morphological and cultural characterization

Agar plugs containing fungal hyphae from the colony margins were transferred to fresh PDA plates for activation, followed by incubation at 25 °C in the dark for 7 days. Morphological characteristics were examined for six isolates. Micromorphological characters from structures produced in culture were observed using a Leica TL3000 Ergo stereomicroscope and Nikon Ci-S microscope. All fungal strains were stored in 10% sterilized glycerin at 4 °C for further studies. Dimensions of microscopic structures, including conidiomata, conidiophores, conidiogenous cells, and conidia, were measured using Digimizer software, with 30 measurements taken for each structure. The plant specimen has been preserved in the herbarium of the Guangxi Medicinal Botanic Garden (**GXMG**). Additionally, the ex-type living cultures were deposited in the China General Microbiological Culture Collection Center (**CGMCC**) and Guangxi University of Chinese Medicine (**GXCM**). The taxonomic information of the new taxa was submitted to Fungal Names (https://nmdc.cn/fungalnames, accessed on 16 Dec. 2025).

DNA extraction, sequencing and phylogenetic analyses

Genomic DNA was extracted from mycelia grown on PDA using a CTAB (cetyltrimethylammonium bromide) method (Guo et al. 2000). The internal transcribed spacer (ITS) region, the large subunit (LSU) rRNA gene, and the translation elongation factor 1-α gene (*tef1*) were amplified using the following primer pairs: ITS1/ITS4 (White et al. 1990), LROR/LR5 (Vilgalys and Hester 1990), and 983F/2218R (Rehner and Buckley 2005), respectively. Amplification was performed in a 25 μl reaction volume, which contained 1.0 μl DNA template, 1.0 μl of each forward and reverse primer, 12.5 μl 2× Master Mix, and

9.5 µl ddH_2O. Polymerase chain reaction (PCR) was per formed under the following conditions: initial denaturation at 94 °C for 5 min, followed by 35 cycles of denaturation at 94 °C for 30 sec, annealing at 48 °C (for ITS and LSU) or 54 °C (for *tef1*) for 50 sec, and extension at 72 °C for 1 min, with a final elongation step at 72 °C for 7 min. The PCR products were then sent to Sangon Biotech (Shanghai, China) Co., Ltd., for sequencing. All sequences were submitted to NCBI's GenBank (https://www.ncbi.nlm.nih.gov, accessed on 26 Nov. 2025) to obtain the GenBank accession numbers. Attempts were also made to amplify *tub2* and *rpb2* loci, but no reliable products were obtained despite optimization of PCR conditions.

The quality of our amplified nucleotide sequences was checked and assembled by SeqMan v.7.1.0 and reference sequences were retrieved from the National Center for Biotechnology Information (NCBI). Phylogenetic analyses were conducted using the PhyloSuite v1.2.3 software (Xiang et al. 2023). Initially, sequences were extracted and aligned using MAFFT v7.505 (Katoh and Standley 2013). The resulting alignments were concatenated into a single dataset. The optimal partitioning strategy and evolutionary models were determined using ModelFinder, employing a greedy search algorithm with linked branch lengths based on the Bayesian Information Criterion (BIC). Phylogenetic trees were constructed using both Maximum Likelihood (ML) and Bayesian Inference (BI) methods. The ML phylogeny was inferred using IQ-TREE (Minh et al. 2020). Nodal support was assessed through 10,000 ultrafast bootstrap replicates using an edge-linked partition style. The BI analysis was performed using MrBayes (Huelsenbeck and Ronquist 2001) with two parallel runs and four Markov chains (one cold, three heated). The analysis ran for 1,000,000 generations, with trees sampled every 1,000 generations. Convergence was confirmed when the average standard deviation of split frequencies (ASDOSF) reached 0.005 (<0.01). The first 25% of sampled trees were discarded as burn-in, and the remaining trees were used to calculate Bayesian posterior probabilities (PP). The resulting trees were generated using FigTree v. 1.4.4 (http://tree.bio.ed.ac.uk/software/figtree, accessed on 28 Nov. 2025) or ITOL: Interactive Tree of Life (https://itol.embl.de, accessed on 28 Nov. 2025) (Letunic and Bork 2024), and the final layout of the trees was refined in Adobe Illustrator CC 2019. All GenBank accession numbers in this study are provided in Table 1.

Results

Phylogenetic analyses

Preliminary molecular identification was conducted via a BLASTn search using the ITS sequences. The results revealed that the isolates obtained in this study exhibited the highest sequence similarity to *Gnomoniopsis fujianensis*, *G. rosae*, *G. smithogilvyi*, *G. hainanensis*, and other closely related taxa. To explicitly verify species boundaries based on the primary fungal barcode, a phylogenetic analysis was performed using the single-locus ITS dataset. The alignment consisted of 58 sequences (including the outgroup *Apiognomonia errabunda* CBS 109747) and comprised 667 characters (including gaps), of which 151 were parsimony-informative, 48 were variable singleton sites, and 468 were constant. The resulting topology (Fig. 1) clearly distinguished the

Table 1. Information of specimens and GenBank accession numbers of the sequences used in the analysis of *Gnomoniopsis* and *Ternstroemiomyces*.

Species	Strains	GenBank accession numbers			References
		ITS	LSU	*tef1*	
Apiognomonia errabunda	CBS 109747	DQ313525	AF408334	EU221914	Sogonov et al. (2007); Sogonov et al. (2008); Castlebury et al. (2002)
Chrysocrypta corymbiae	CBS 132528*	NA	MH878334	MH545457	Vu et al. (2019)
Coniella africana	CBS 114133*	AY339344	AY339293	NA	Van Niekerk et al. (2004)
Coniella straminea	CBS 149.22	AY339348	AY339296	NA	Van Niekerk et al. (2004)
Cryphonectria naterciae	CBS 129351	MH865223	MH876660	MN271844	Vu et al. (2019); Jiang et al. (2020a)
Cryphonectria parasitica	ATCC 38755	AY141856	EU199123	EU222014	Liu et al. (2003); Sogonov et al. (2008)
Dendrostoma atlanticum	CBS 145804*	MN447223	NA	MN432167	Jaklitsch and Voglmayr (2019)
D. aurorae	CFCC 52753*	MH542498	MH542646	MH545447	Jiang et al. (2019)
D. aurorae	CFCC 52754	MH542499	MH542647	MH545448	Jiang et al. (2019)
D. castaneae	CFCC 52745*	MH542488	MH542644	MH545437	Jiang et al. (2019)
D. castaneae	CFCC 52746	MH542489	NA	MH545438	Jiang et al. (2019)
D. castaneicola	CFCC 52743*	MH542496	NA	MH545445	Jiang et al. (2019)
D. castaneicola	CFCC 52744	MH542497	NA	MH545446	Jiang et al. (2019)
D. castaneum	CBS 145803*	MN447225	NA	MN432169	Jaklitsch and Voglmayr (2019)
D. chinense	CFCC 52755*	MH542500	MH542648	MH545449	Jiang et al. (2019)
D. chinense	CFCC 52756	MH542501	MH542649	MH545450	Jiang et al. (2019)
D. covidicola	GZCC 20-0355*	MW261327	MW261325	MW262894	Samarakoon et al. (2021)
D. creticum	CBS 145802*	MN447228	NA	MN432171	Jaklitsch and Voglmayr (2019)
D. dispersum	CFCC 52730	MH542467	MH542629	MH545416	Jiang et al. (2019)
D. dispersum	CFCC 52728*	MH542469	MH542631	MH545418	Jiang et al. (2019)
D. donglinensis	CFCC 53148*	MN266206	MN265880	MN315480	Zhu et al. (2019)
D. donglinensis	CFCC 53149	MN266207	MN265881	MN315481	Zhu et al. (2019)
D. elaeocarpi	CFCC 53113*	MK432638	MK429908	MK578114	Chen et al. (2022)
D. elaeocarpi	CFCC 53114	MK432639	MK429909	MK578115	Chen et al. (2022)
D. istriacum	CBS 145801*	MN447229	NA	MN432172	Jaklitsch and Voglmayr (2019)
D. leiphaemia	CFCC 54038*	MN545571	NA	MN551288	Chen et al. (2022)
D. leiphaemia	CFCC 54039	MN545572	NA	MN551289	Chen et al. (2022)
D. luteum	IMI506898*	MN648726	MN648728	MN812768	Crous et al. (2020)
D. mali	CFCC 52102*	MG682072	MG682012	MG682052	Fan et al. (2018)
D. osmanthi	CFCC 52106*	MG682073	MG682013	MG682053	Fan et al. (2018)
D. osmanthi	CFCC 52108	MG682074	MG682015	MG682054	Fan et al. (2018)
D. parasiticum	CFCC 52762*	MH542482	MH542638	MH545431	Jiang et al. (2019)
D. parasiticum	CFCC 52764	MH542483	MH542639	MH545432	Jiang et al. (2019)
D. qinlingense	CFCC 52732*	MH542471	MH542633	MH545420	Jiang et al. (2019)
D. qinlingense	CFCC 52733	MH542472	MH542634	MH545421	Jiang et al. (2019)
D. quercinum	CFCC 52103*	MG682077	MG682017	MG682057	Fan et al. (2018)
D. quercinum	CFCC 52104	MG682078	MG682018	MG682058	Fan et al. (2018)
D. quercus	CFCC 52739*	MH542476	MH542635	MH545425	Jiang et al. (2019)
D. quercus	CFCC 52738	MH542477	NA	MH545426	Jiang et al. (2019)
D. rizhaoense	CFCC 57559*	PP965514	NA	PP957893	Jiang et al. (2024)
D. rizhaoense	CFCC 57560	PP965515	NA	PP957894	Jiang et al. (2024)
D. shaanxiense	CFCC 52741*	MH542486	MH542642	MH545435	Jiang et al. (2019)
D. shaanxiense	CFCC 52742	MH542487	MH542643	MH545436	Jiang et al. (2019)
D. shandongense	CFCC 52759*	MH542504	MH542652	MH545453	Jiang et al. (2019)
D. shandongense	CFCC 52760	MH542505	MH542653	MH545454	Jiang et al. (2019)
D. tianii	CFCC 58140*	PP965516	NA	PP957895	Jiang et al. (2024)
D. tianii	CFCC 58141	PP965517	NA	PP957896	Jiang et al. (2024)
Diaporthella corylina	CBS 121124	KC343004	NA	KC343730	Gomes et al. (2013)

Species	Strains	GenBank accession numbers			References
		ITS	LSU	*tef1*	
Diaporthella cryptica	CBS 140348	MN172409	MN172390	MN271854	Jiang et al. (2020a)
Disculoides calophyllae	CBS 142080*	KY979745	KY979800	NA	Crous et al. (2013)
Disculoides corymbiae	CBS 142076*	KY173403	KY173495	NA	Crous et al. (2013)
Disculoides eucalypti	CBS 132183*	MH866015	MH877462	MH545455	Vu et al. (2019)
Disculoides eucalyptorum	CBS 132184*	MH866016	MH877463	MH545456	Vu et al. (2019)
Disculoides fraxinoides	CBS 143430*	MN161909	MN162183	NA	Crous et al. (2019)
Dwiroopa lythri	CBS 109755	MK510675	AF408364	NA	Castlebury et al. (2002); Xavier et al. (2019)
Dwiroopa punicae	CBS 143163*	MK510676	MK510686	NA	Xavier et al. (2019)
Dwiroopa punicae	A7	MK510681	MK510687	NA	Xavier et al. (2019)
Erythrogloeum hymenaeae	CPC 18819	JQ685519	JQ685525	NA	Crous et al. (2012a)
Foliocryphia eucalypti	CBS 124779*	GQ303276	GQ303307	MN271861	Cheewangkoon et al. (2009); Jiang et al. (2020a)
Foliocryphia eucalyptorum	CBS 142536*	KY979772	KY979827	MN271862	Crous et al. (2013); Jiang et al. (2020a)
Gnomoniopsis alderdunensis	CBS 125680*	GU320825	MH875097	GU320801	Walker et al. (2010); Vu et al. (2019)
G. alderdunensis	CBS 125681	GU320827	MH875098	GU320802	Walker et al. (2010); Vu et al. (2019)
G. annonae	CGMCC3.28195*	PQ325623	NA	PQ336654	Zhang et al. (2025)
G. annonae	SAUCC6333	PQ325624	NA	PQ336655	Zhang et al. (2025)
G. castaneae	GCAS5	MH107830	MZ682110	MH213486	Tziros (2019)
G. chamaemori	CBS 804.79*	GU320817	NA	GU320809	Walker et al. 2010
G. chinensis	CFCC 52286*	MG866032	NA	MH545370	Jiang et al. (2020b)
G. chinensis	CFCC 52288	MG866034	NA	MH545372	Jiang et al. (2020b)
G. clavulata	CBS 121255	EU254818	NA	EU221934	Sogonov et al. (2008)
G. comari	CBS 806.79	EU254821	EU255114	GU320810	Sogonov et al. (2008); Walker et al. (2010)
G. daii	CFCC 54043*	MZ902911	NA	MZ936387	Jiang et al. (2021)
G. daii	CFCC 55517	MZ902912	NA	MZ936388	Jiang et al. (2021)
G. diaoluoshanensis	SAUCC DL0963*	ON753744	NA	ON759769	Wang et al. (2022b)
G. diaoluoshanensis	SAUCC DL0964	ON753743	NA	ON759768	Wang et al. (2022b)
G. fagacearum	CFCC 54316*	MZ902916	NA	MZ936392	Jiang et al. (2021)
G. flava	CFCC 71563*	PV257808	NA	PV268106	Li et al. (2025b)
G. flava	CFCC 71566	PV257809	NA	PV268107	Li et al. (2025b)
G. fructicola	CBS 208.34	EU254826	EU255116	EU221968	Sogonov et al. (2008)
G. fructicola	CBS 121226	EU254824	NA	EU221961	Sogonov et al. (2008)
G. fujianensis	CGMCC3.28229*	PQ325641	NA	PQ336672	Zhang et al. (2025)
G. fujianensis	SAUCC1260	PQ325642	NA	PQ336673	Zhang et al. (2025)
G. guangdongensis	CFCC 54443*	MZ902918	NA	MZ936394	Jiang et al. (2021)
G. guangdongensis	CFCC 54331	MZ902919	NA	MZ936395	Jiang et al. (2021)
G. guttulata	MS 0312	EU254812	NA	NA	Sogonov et al. (2008)
G. hainanensis	CFCC 54376*	MZ902921	NA	MZ936397	Jiang et al. (2021)
G. hainanensis	CFCC 55877	MZ902922	NA	MZ936398	Jiang et al. (2021)
G. idaeicola	CBS 125672	GU320823	NA	GU320797	Walker et al. (2010)
G. idaeicola	CBS 125673	GU320824	NA	GU320798	Walker et al. (2010)
G. juglandis	CGMCC3.28233*	PQ325637	NA	PQ336668	Zhang et al. (2025)
G. juglandis	SAUCC2375	PQ325638	NA	PQ336669	Zhang et al. (2025)
G. lithocarpi	SAUCC YN0743*	ON753749	NA	ON759765	Wang et al. (2022b)
G. lithocarpi	SAUCC YN0742	ON753750	NA	ON759764	Wang et al. (2022b)
G. luodingensis	**CGMCC 3.29462* = GXCM RG106**	**PX611876**	**PX611993**	**PX655142**	**This study**
G. luodingensis	**GXCM RG119**	**PX611877**	**NA**	**PX655141**	**This study**
G. macounii	CBS 121468	EU254762	EU255087	EU221979	Sogonov et al. (2008)
G. mengyinensis	SAUCC MY0293*	ON753741	NA	ON759766	Wang et al. (2022b)
G. mengyinensis	SAUCC MY0296	ON753742	NA	ON759767	Wang et al. (2022b)
G. occulta	CBS 125677	GU320828	MH875094	GU320812	Walker et al. (2010); Vu et al. (2019)

Species	Strains	GenBank accession numbers			References
		ITS	LSU	*tef1*	
G. occulta	CBS 125678	GU320829	MH875095	GU320800	Walker et al. (2010); Vu et al. (2019)
G. paraclavulata	CBS 123202	GU320830	NA	GU320815	Walker et al. (2010)
G. racemula	CBS 121469*	EU254841	EU255122	EU221889	Sogonov et al. (2008)
G. rosae	CBS 145085*	MK047451	MK047501	NA	Crous et al. (2018)
G. rosae	GUCC 408.7	OP581231	OP581244	OP688536	Wang et al. (2022a)
G. saprophytica	CGMCC3.28192*	PQ325633	NA	PQ336664	Zhang et al. (2025)
G. saprophytica	SAUCC3342	PQ325634	NA	PQ336665	Zhang et al. (2025)
G. sanguisorbae	CBS 858.79	GU320818	NA	GU320805	Walker et al. (2010)
G. silvicola	CFCC 54304	MZ902925	NA	MZ936401	Jiang et al. (2021)
G. silvicola	CFCC 54418*	MZ902926	NA	MZ936402	Jiang et al. (2021)
G. smithogilvyi	CBS 130190*	JQ910642	MH877031	JQ910645	Crous et al. (2012c); Vu et al. (2019)
G. smithogilvyi	CBS 130189	JQ910644	MH877030	JQ910647	Crous et al. (2012c); Vu et al. (2019)
G. taishanensis	CGMCC3.28230*	PQ325645	NA	PQ336676	Zhang et al. (2025)
G. taishanensis	SAUCC1033	PQ325646	NA	PQ336677	Zhang et al. (2025)
G. tormentillae	CBS 904.79	EU254856	EU255133	GU320795	Sogonov et al. (2008); Walker et al. (2010)
G. xishuangbannaensis	CGMCC3.25980*	PQ325643	NA	PQ336674	Zhang et al. (2025)
G. xishuangbannaensis	CGMCC3.25979	PQ325644	NA	PQ336675	Zhang et al. (2025)
G. yunnanensis	SAUCC YN1659*	ON753746	NA	ON759771	Wang et al. (2022b)
G. yunnanensis	SAUCC YN1657	ON753747	NA	ON759772	Wang et al. (2022b)
Harknessia eucalypti	CBS 342.97	AY720745	NA	MN271866	Lee et al. (2004); Jiang et al. (2020a)
Harknessia eucalyptorum	CPC 14951	JQ706093	JQ706218	NA	Crous et al. (2012b)
Harknessia leucospermi	CBS 775.97*	AY720727	AY720824	MN271871	Lee et al. (2004); Jiang et al. (2020a)
Harknessia malayensis	CBS 142544	KY979789	KY979844	NA	Crous et al. (2013)
Harknessia syzygii	CPC 184*	AY720738	AY720834	NA	Lee et al. (2004)
Ternstroemiomyces machili	CGMCC 3.28263*	PQ287929	PQ285099	PQ305855	Zhang et al. (2025)
Te. ternstroemiae	CGMCC 3.28237*	PQ287931	PQ285101	PQ305857	Zhang et al. (2025)
Te. cinnamomi	**CGMCC 3.29461* = GXCM RG130**	**PX611875**	**PX611994**	**PX655144**	**This study**
Te. cinnamomi	**GXCM RG126**	**PX611874**	**PX617115**	**PX655143**	**This study**
Te. zhaoqingensis	**CGMCC 3.29460* = GXCM RG79**	**PX611873**	**PX611992**	**PX655140**	**This study**
Te. zhaoqingensis	**GXCM RG78**	**PX611872**	**PX611991**	**PX655139**	**This study**

Notes: Newly generated sequences are in bold. The ex-type, ex-epitype and ex-neotype strains are marked with *.

new isolates as a separate lineage. Specifically, the new species *Gnomoniopsis luodingensis* formed a well-separated branch with maximum support in the single-locus analysis. Within this clade, strain GXCM RG119 showed a slight branch length variation due to 3 base pair differences (99.5% identity) compared to the GXCM RG106, representing intraspecific variation.

Subsequently, to establish a robust evolutionary framework and resolve potential long-branch attraction artifacts observed in preliminary analyses, a concatenated multilocus dataset comprising ITS, LSU, and *tef1* sequences was constructed. The final alignment consisted of 58 sequences and 1852 characters (ITS: 1–458; LSU: 459–1329; *tef1*: 1330–1852), of which 1404 were constant, 76 were variable singleton sites, and 372 were parsimony-informative. The topologies inferred from Maximum Likelihood (ML) and Bayesian Inference (BI) analyses, utilizing the best-fit models K2P+I+G4 for ITS, K2P+I for LSU, and HKY+F+I+G4 for *tef1*, were congruent with the single-locus results. As shown in Fig. 2, *Gnomoniopsis luodingensis* formed a distinct, fully supported monophyletic clade. The analysis revealed that the new species is phylogenetically closely related to *G. hainanensis*, *G. fujianensis*, and *G. fagacearum*, yet represents a clearly distinct lineage.

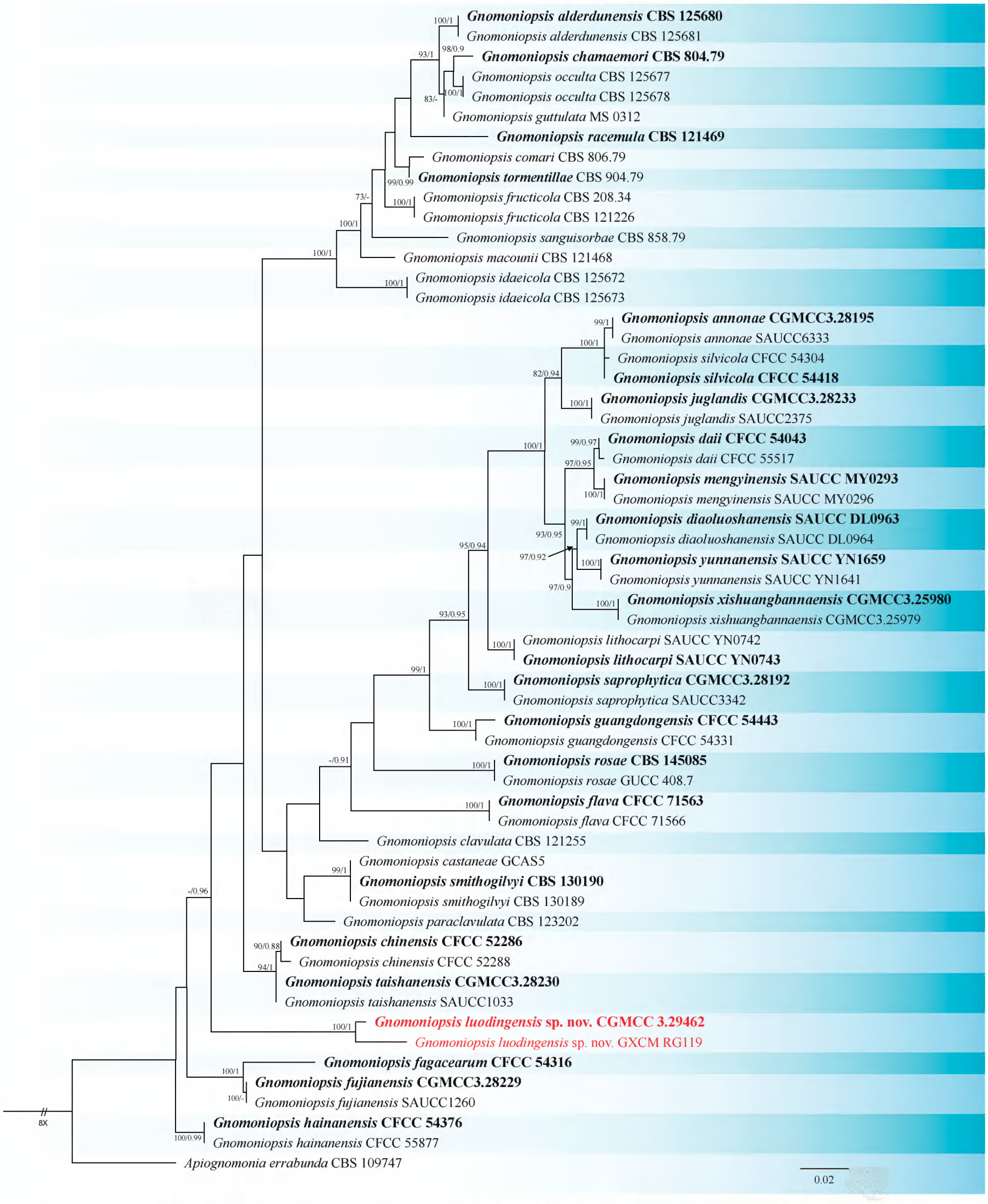

Figure 1. Phylogram of *Gnomoniopsis* species generated from a Maximum Likelihood analysis based on the ITS sequence dataset. The tree is rooted with *Apiognomonia errabunda* (CBS 109747). Bootstrap support values ≥ 70% and Bayesian posterior probabilities ≥ 0.90 are demonstrated at the branches. Isolates from the present study are indicated in red. Ex-type or ex-holotype strains are indicated in bold black. Some branches are shortened according to the indicated multipliers to fit the page size, and these are indicated by the symbol (//).

Preliminary molecular identification was conducted via a BLASTn search using the ITS sequences. The results revealed that the isolates obtained in this study exhibited the highest sequence similarity to *Ternstroemiomyces ternstroemiae* and *Te. machili* (Ternstroemiomycetaceae), as well as taxa

within the family Erythrogloeaceae. To explicitly verify species boundaries, a phylogenetic analysis was performed using the single-locus ITS dataset. The alignment consisted of 69 sequences, with *Diaporthella corylina* (CBS 121124) and *Diaporthella cryptica* (CBS 140348) selected as the outgroup. The resulting topology clearly (Fig. 3) distinguished the new isolates as distinct lineages.

Subsequently, to establish a robust evolutionary framework, a concatenated multilocus dataset comprising ITS, LSU, and *tef1* sequences was constructed. The final alignment consisted of 70 sequences and 1584 characters (ITS: 1–434; LSU: 435–1250; *tef1*: 1251–1584), of which 1119 were constant, 95 were variable singleton sites, and 370 were parsimony-informative. The topologies inferred from Maximum Likelihood (ML) and Bayes-

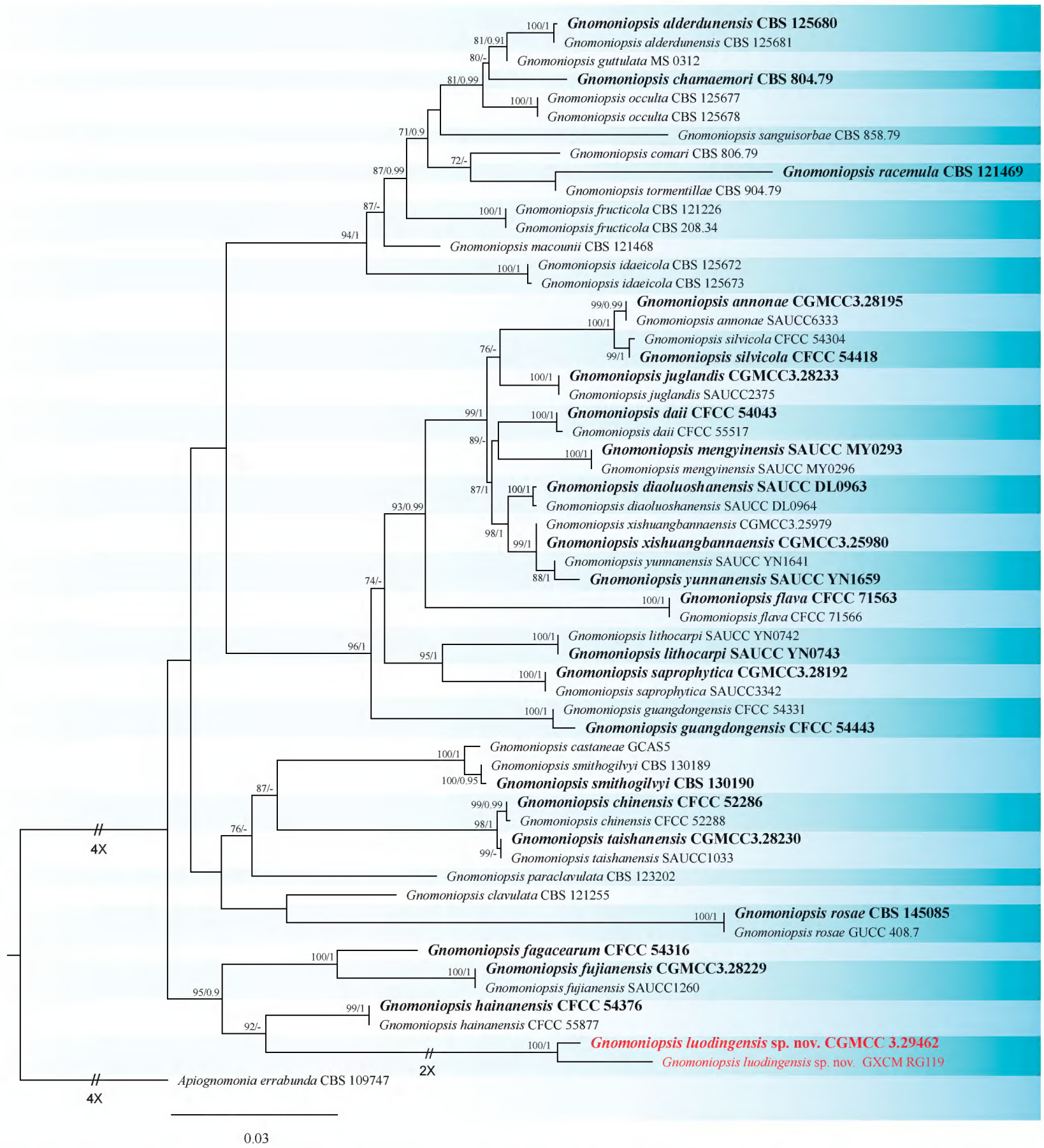

Figure 2. Phylogram of *Gnomoniopsis* species generated from a Maximum Likelihood analysis based on the combined ITS, LSU, and *tef1* sequence dataset. The tree is rooted with *Apiognomonia errabunda* (CBS 109747). Bootstrap support values ≥ 70% and Bayesian posterior probabilities ≥ 0.90 are demonstrated at the branches. Isolates from the present study are indicated in red. Ex-type or ex-holotype strains are indicated in bold black. Some branches are shortened according to the indicated multipliers to fit the page size, and these are indicated by the symbol (//).

ian Inference (BI) analyses, utilizing the best-fit models TIM3e+I+G4 for ITS and *tef1*, and GTR+F+I+G4 for LSU, were congruent with the single-locus results. As shown in Fig. 4, the phylogenetic analysis revealed that the isolates represent two distinct novel species, herein described as *Ternstroemiomyces cinnamomi* and *Ternstroemiomyces zhaoqingensis*. Both species formed independent, fully supported monophyletic clades. Notably, the two new species clustered together with strong support and formed a sister group to the clade containing *Te. ternstroemiae* and *Te. machili*.

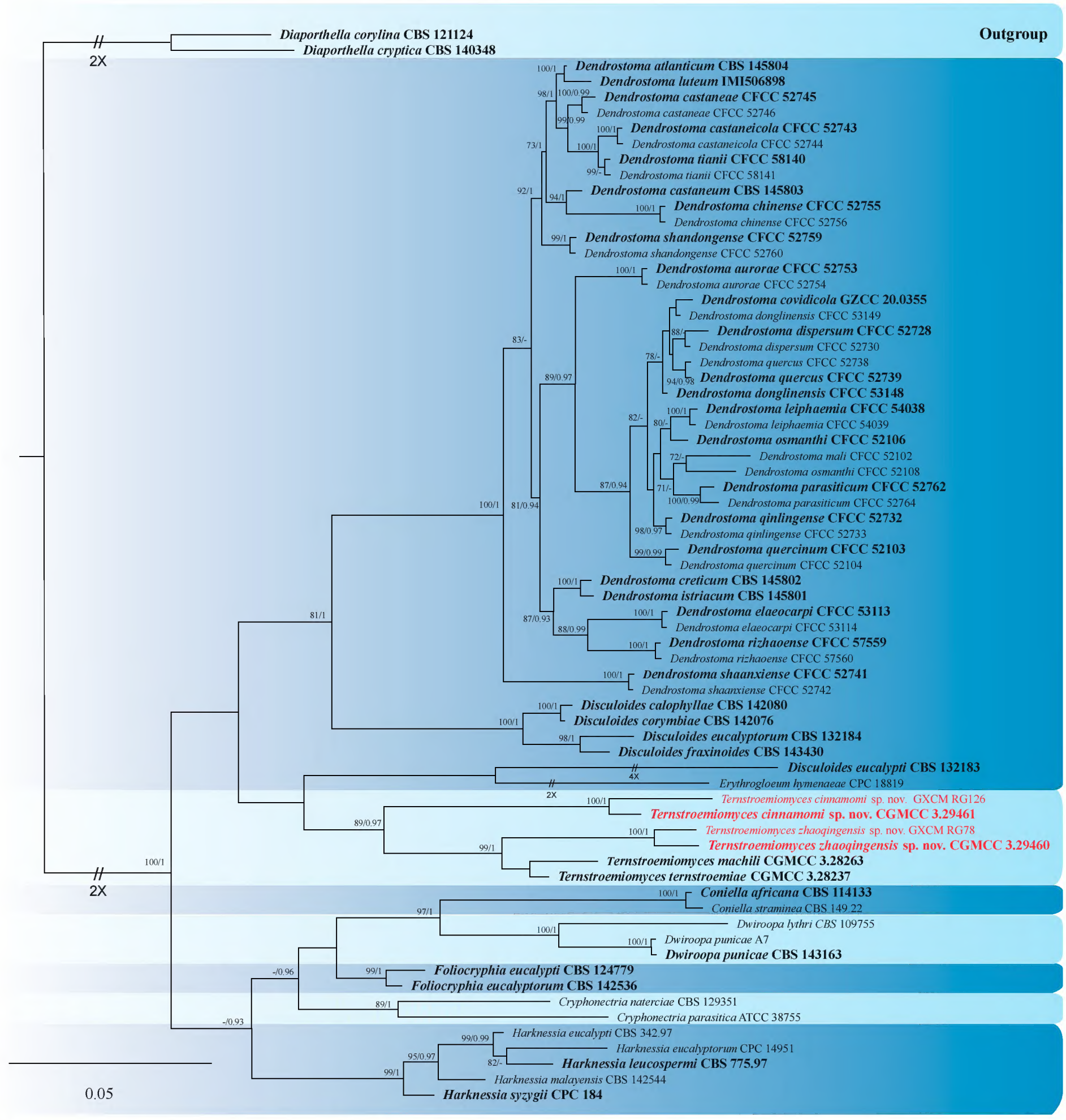

Figure 3. Phylogram of Ternstroemiomyces species generated from a Maximum Likelihood analysis based on the ITS sequence dataset. The tree is rooted with *Diaporthella corylina* (CBS 121124) and *Diaporthella cryptica* (CBS 140348). Bootstrap support values ≥ 70% and Bayesian posterior probabilities ≥ 0.90 are demonstrated at the branches. Isolates from the present study are indicated in red. Ex-type or ex-holotype strains are indicated in bold black. Some branches are shortened according to the indicated multipliers to fit the page size, and these are indicated by the symbol (//).

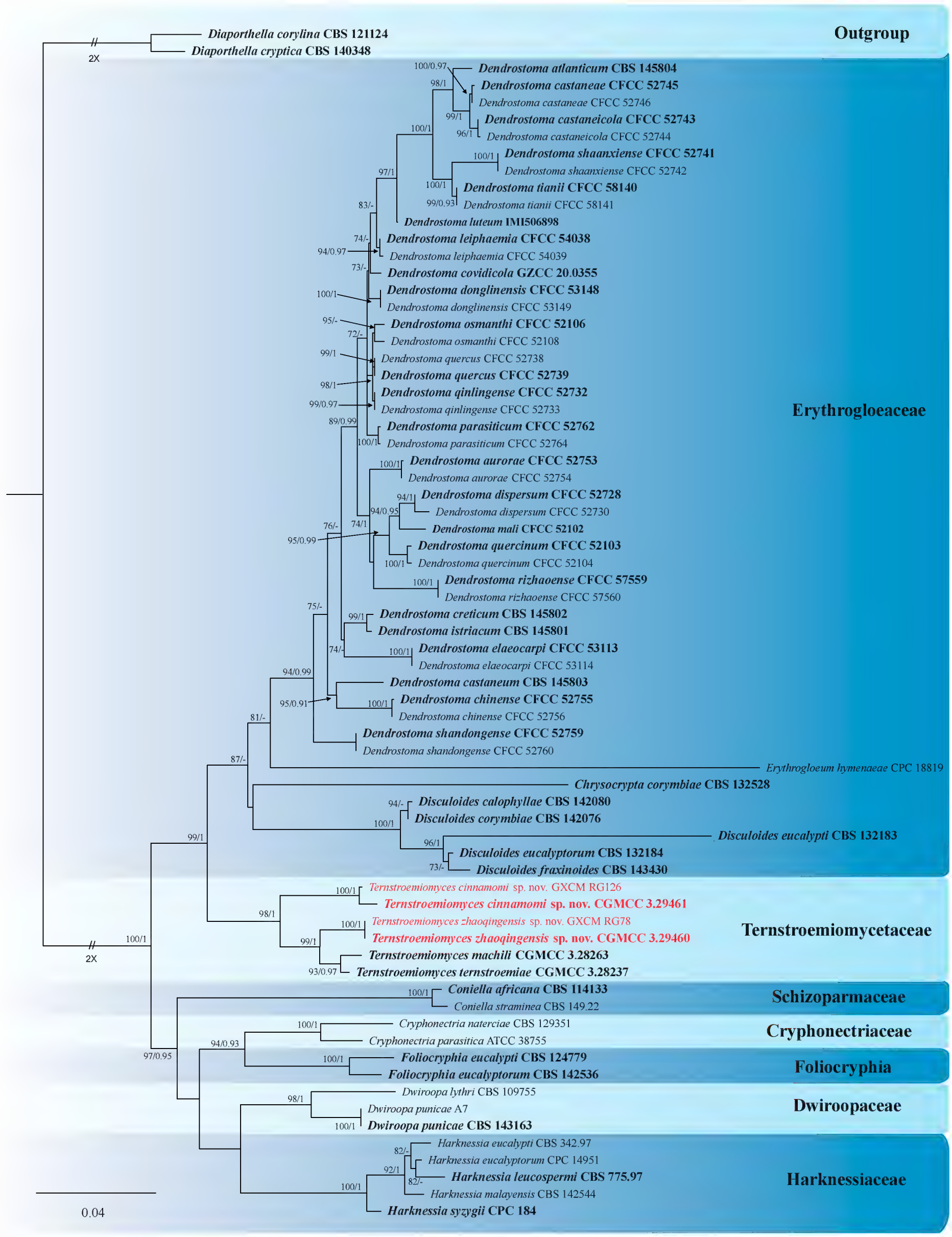

Figure 4. Phylogram of *Ternstroemiomyces* species generated from a Maximum Likelihood analysis based on the combined ITS, LSU, and *tef1* sequence dataset. The tree is rooted with *Diaporthella corylina* (CBS 121124) and *Diaporthella cryptica* (CBS 140348). Bootstrap support values ≥ 70% and Bayesian posterior probabilities ≥ 0.90 are demonstrated at the branches. Isolates from the present study are indicated in red. Ex-type or ex-holotype strains are indicated in bold black. Some branches are shortened according to the indicated multipliers to fit the page size, and these are indicated by the symbol (//).

Taxonomy

***Gnomoniopsis luodingensis* Z.H. Guo & X.M. Tan, sp. nov.**
Fungal Names: FN 573162
Fig. 5

Holotype. CHINA • Guangdong Province, Luoding City, on leaves of *Cinnamomum cassia* (Lauraceae), 22°57'90"N, 111°69'98"E, 353.2 m asl., November. 2022, X.M. Tan, holotype GXMG 20221110-1, ex-type living culture GXCM RG106 = CGMCC 3.29462.

Etymology. Named after the collection site of the type specimen, Luoding City.

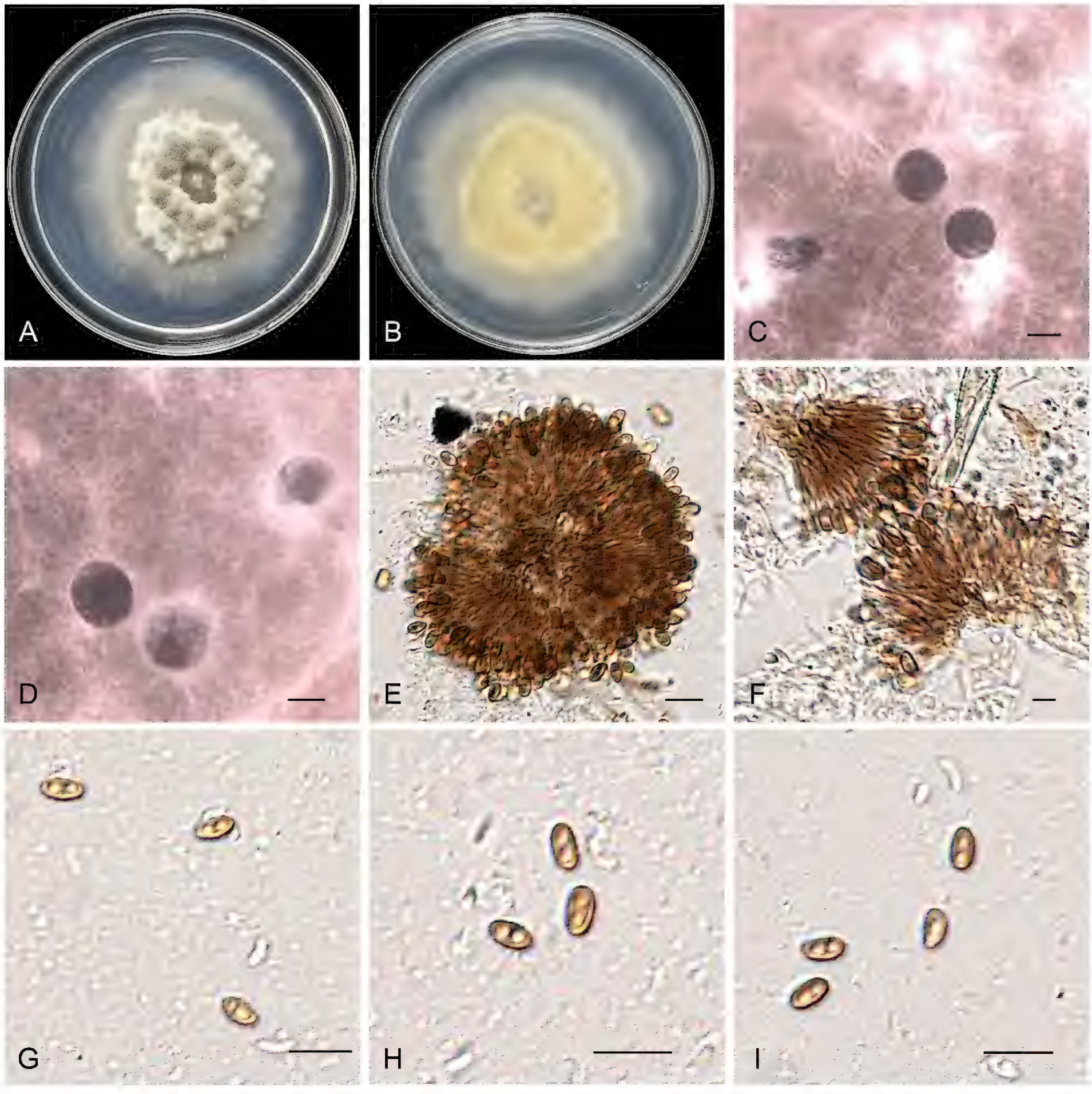

Figure 5. *Gnomoniopsis luodingensis* (CGMCC 3.29462). **A, B.** Inverse and reverse sides of colony after seven days on PDA; **C, D.** Conidiomata forming on PDA; **E, F.** Conidiophores and conidiogenous cells with developing conidia; **G–I.** Conidia. Scale bars: 500 μm (**C, D**); 10 μm (**E–I**).

Description. Endophytic in leaves of *Cinnamomum cassia*. Colonies on PDA at 25 °C in darkness, attaining 67–70 mm diam. after seven days, with moderate aerial mycelia, grey in the center, white at the edge, and light yellow in reverse. Asexual morph: ***Conidiomata*** pycnidial 450–550 µm, half-buried in the culture medium, black, scattered, globose to subglobose, exuding conidia droplets from central ostioles in dark at 25 °C. ***Conidiophores*** 18–22 × 1.3–2.6 µm, slender and rod-shaped, radiating slightly outward from the base, smooth, swollen apex. ***Conidiogenous cells*** 4–5.5 × 2.5–3 µm, brown, smooth, cylindrical to ampulliform, attenuate towards apex, phialidic. ***Conidia*** 4.2–5.8 × 2.6–3.2 µm, formed singly, oblong to ellipsoid, brown, smooth, thin-walled, apex obtuse, with an inconspicuous base. Sexual morph was not observed.

Notes. Phylogenetic analysis based on the combined dataset showed that *Gnomoniopsis luodingensis* formed a distinct and fully supported lineage (BP/PP: 100/1). It appeared as the sister species to *G. hainanensis* with high bootstrap support (BP: 92%), and together they clustered with *G. fujianensis* and *G. fagacearum* in a well-supported clade (BP/PP: 95/0.9). *G. luodingensis* (CGMCC 3.29462) was distinguished from *Gnomoniopsis hainanensis* (CFCC 54376), *G. fujianensis* (CGMCC3.28229), and *G. fagacearum* (CFCC 54316) by 28/494, 27/548, 29/496 pair differences in ITS sequences. *G. luodingensis* is different from the phylogenetically close species *G. hainanensis* by its conidial size and length-width ratio (4.2–5.8 × 2.6–3.2 µm, L/W = 1.6–2.2 in *G. luodingensis* vs. 7.3–12.2 × 3.3–4.2 µm, L/W = 1.9–3.3 in *G. hainanensis*). A synopsis of morphological characteristics compared with other closely related species is presented in Table 2. Therefore, we introduce this taxon as a new species.

Table 2. Synopsis of morphological characteristics of *Gnomoniopsis luodingensis* compared with closely related species.

Species	Conidiomata (µm)	Conidial Length (µm)	Conidial Width (µm)	L/W Ratio	Reference
G. fagacearum	250–450	(9–) 9.6–11.4 (–12.6)	(2.8–) 3.1–4 (–4.5)	2.1–4.2	Jiang et al. (2021)
G. fujianensis	100–200	4.8–7.5	1.7–2.5	NA	Zhang et al. (2025)
G. hainanensis	100–300	(7.3–) 8–10 (–12.2)	(3.3–) 3.4–3.9 (–4.2)	1.9–3.3	Jiang et al. (2021)
G. luodingensis	450–550	4.2–5.8	2.6–3.2	1.6–2.2	This study

Ternstroemiomyces cinnamomi **Z.H. Guo & X.M. Tan, sp. nov.**

Fungal Names: FN 573163

Fig. 6

Holotype. China • Guangdong Province, Zhaoqing City, on leaves of *Cinnamomum cassia* (Lauraceae), 23°13'97"N, 112°04'48"E, 57.3 m asl., October. 2022, X.M. Tan, holotype GXMG 20221025-1, ex-type living culture GXCM RG130 = CGMCC 3.29461.

Etymology. The epithet "*cinnamomi*" refers to the generic name of the host plant *Cinnamomum cassia*.

Description. Endophytic in leaves of *Cinnamomum cassia*. Colonies on PDA at 25 °C in darkness, attaining 59–64 mm diam. after seven days, colonies spreading out like petals, white with moderate mycelia, undulate margin, and circular outward extension, reverse similar in color. Asexual morph: ***Conidiomata*** pycnidial, 350–500 µm, buried or attached to mycelia, brown (later turning black), aggregated or solitary, erumpent, exuding hyaline conidia. ***Conidiophores***

indistinct, often reduced. ***Conidiogenous cells*** 8.5–10 × 3.5–5.5 µm, hyaline, cylindrical to ampulliform, attenuate towards the apex, exhibiting a transparent appearance with a narrowed phialidic neck. ***Conidia*** 10.5–14.5 × 5–7.6 µm, pale brown, smooth, multi-guttulate, range from oblong to ellipsoid, base truncate, with a truncate base and a conspicuous hilum measuring 1–1.8 µm. Sexual morph was not observed.

Notes. Phylogenetic analysis (Fig. 4) based on the combined dataset showed that *Ternstroemiomyces cinnamomi* formed a distinct and fully supported lineage (BP/PP: 100/1). It appeared as the sister lineage to the clade comprising *Te. zhaoqingensis*, *Te. machili* and *Te. ternstroemiae*, and together they clustered in a well-supported clade (BP/PP: 98/1). *Te. cinnamo-*

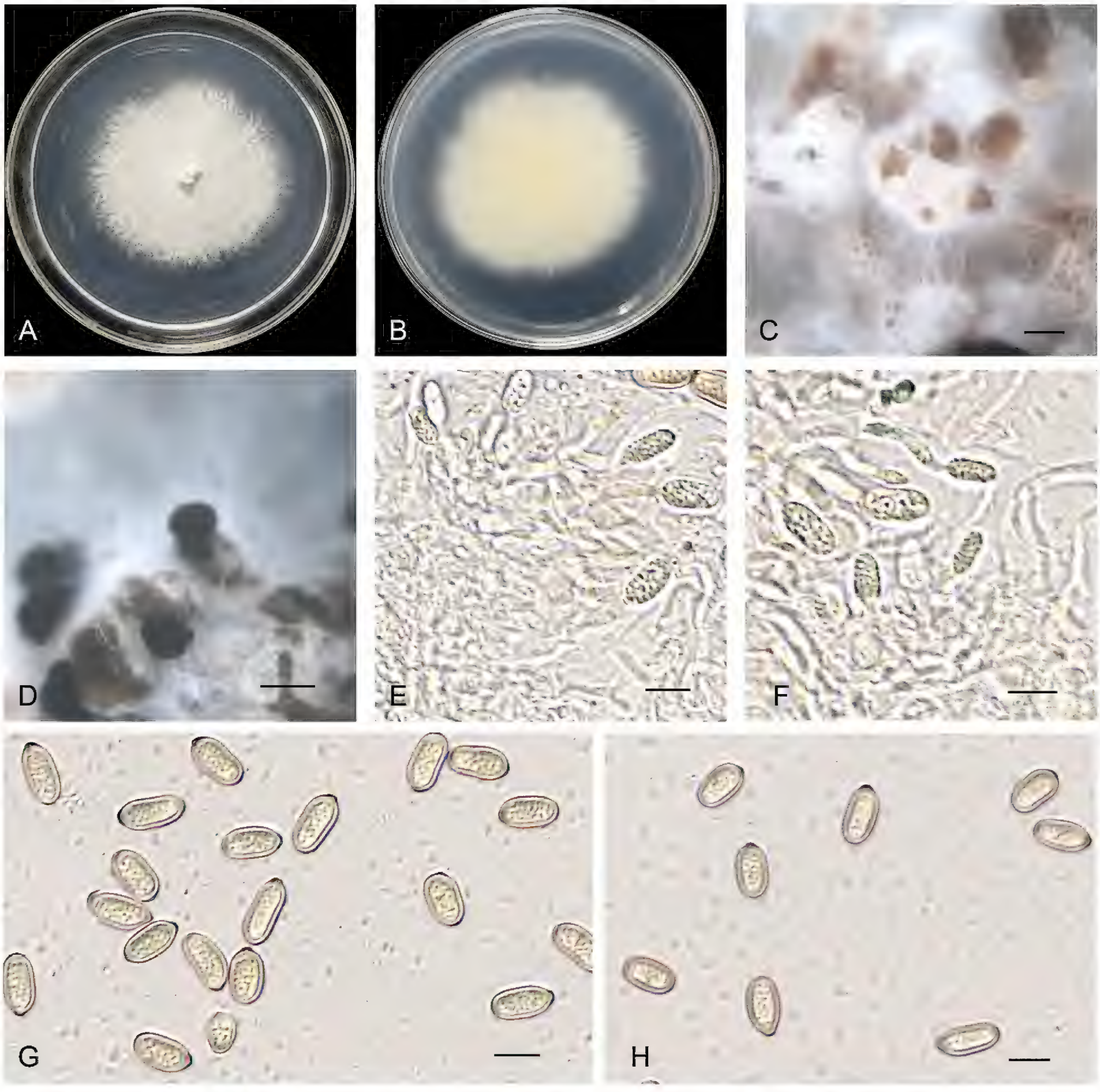

Figure 6. *Ternstroemiomyces cinnamomi* (CGMCC 3.29461). **A, B.** Inverse and reverse sides of colony after seven days on PDA; **C, D.** Conidiomata forming on PDA; **E, F.** Conidiophores and conidiogenous cells with developing conidia; **G, H.** Conidia. Scale bars: 500 µm (**C, D**); 10 µm (**E–H**).

mi (CGMCC 3.29461) was distinguished from *Te. zhaoqingensis* (CGMCC 3.29460) by 51/574, 8/875, and 22/971 base pairs differences in ITS, LSU, and *tef1* sequences, from *Te. ternstroemiae* (CGMCC 3.28237) by 39/549 and 4/843 base pair, from *Te. machili* (CGMCC 3.28263) by 43/551 and 6/840 base pair differences in ITS and LSU sequences, respectively. Morphologically, *Te. zhaoqingensis* lacks an asexual sporulation description, making it impossible to compare microscopic structures with *Te. cinnamomi*. However, their macroscopic colony colors differ greatly: on PDA, *Te. cinnamomi* is uniform white while *Te. zhaoqingensis* is yellowish-white at the center with white edges. Morphologically, since *Te. zhaoqingensis* only had a description of sexual morphology, it could not be directly compared with the asexual morphology in this study. Then, *Te. ternstroemiae* and *Te. machili* (Zhang et al. 2025), which were closely related on the evolutionary tree, were selected for comparison. A synopsis of morphological characteristics of *Te. cinnamomi* compared with these closely related species is presented in Table 3. The conidia of *Te. cinnamomi* (10.5–14.5 × 5–7.6 μm) were smaller than *Te. ternstroemiae* (18–22(–25) × 8.7–10 μm), and *Te. machili* (11–18.5 × 8.2–10.5 μm). The new isolates were described here as *Ternstroemiomyces cinnamomi* sp. nov., based on their distinct morphological characteristics and phylogenetic analysis.

***Ternstroemiomyces zhaoqingensis* Z.H. Guo & X.M. Tan, sp. nov.**

Fungal Names: FN 573164

Fig. 7

Holotype. China • Guangdong Province, Zhaoqing City, on leaves of *Cinnamomum cassia* (Lauraceae), 23°13'97" N, 112°04'48" E, 57.3 m asl., October. 2022, X.M. Tan, holotype GXMG 20221025-2, ex-type living culture GXCM RG79 = CGMCC 3.29460.

Etymology. Named after the collection site of the type specimen, Zhaoqing City.

Description. Endophytic in leaves of *Cinnamomum cassia*. Colonies on PDA at 25 °C in darkness, attaining 61–64 mm diam. after seven days, colonies spreading out like petals, yellowish-white with dense mycelia, undulate margin and circular outward extension, reverse similar in color. Sexual morph: ***Ascomata*** 200–350 μm, buried or attached to the surface of mycelia, aggregative or solitary, globose to elliptical, brown, exuding hyaline asci. ***Asci*** 66.1–89.7 × 5.2–10.3 μm, unitunicate, 8-spored, subcylindrical to long obovoid, wedge-shaped. ***Ascospores*** 11.5–18.1 × 4.8–6.8 μm, long-ellipsoidal to sub-lageniform, sharpening to apex, hyaline, median 1-septate. Asexual morph not observed.

Notes. Phylogenetic analysis based on the combined dataset showed that *Ternstroemiomyces zhaoqingensis* formed a distinct and fully supported lineage (BP/PP: 100/1). It appeared as the sister lineage to *Te. machili* and *Te. ternstroemiae* with high support (BP/PP: 99/1), and together they clustered with *Te. cinnamomi* in a well-supported clade (BP/PP: 98/1) (Fig. 2). *Te. zhaoqingensis* was distinguished from *Te. ternstroemiae* (CGMCC 3.28237) by 21/549, and 7/843 base pair, from *Te. machili* (CGMCC 3.28263) by 28/550, and 9/840 base pair differences in ITS and LSU, sequences, respectively. Morphologically, *Te. zhaoqingensis* did not produce asexual sporulation under the conditions examined,

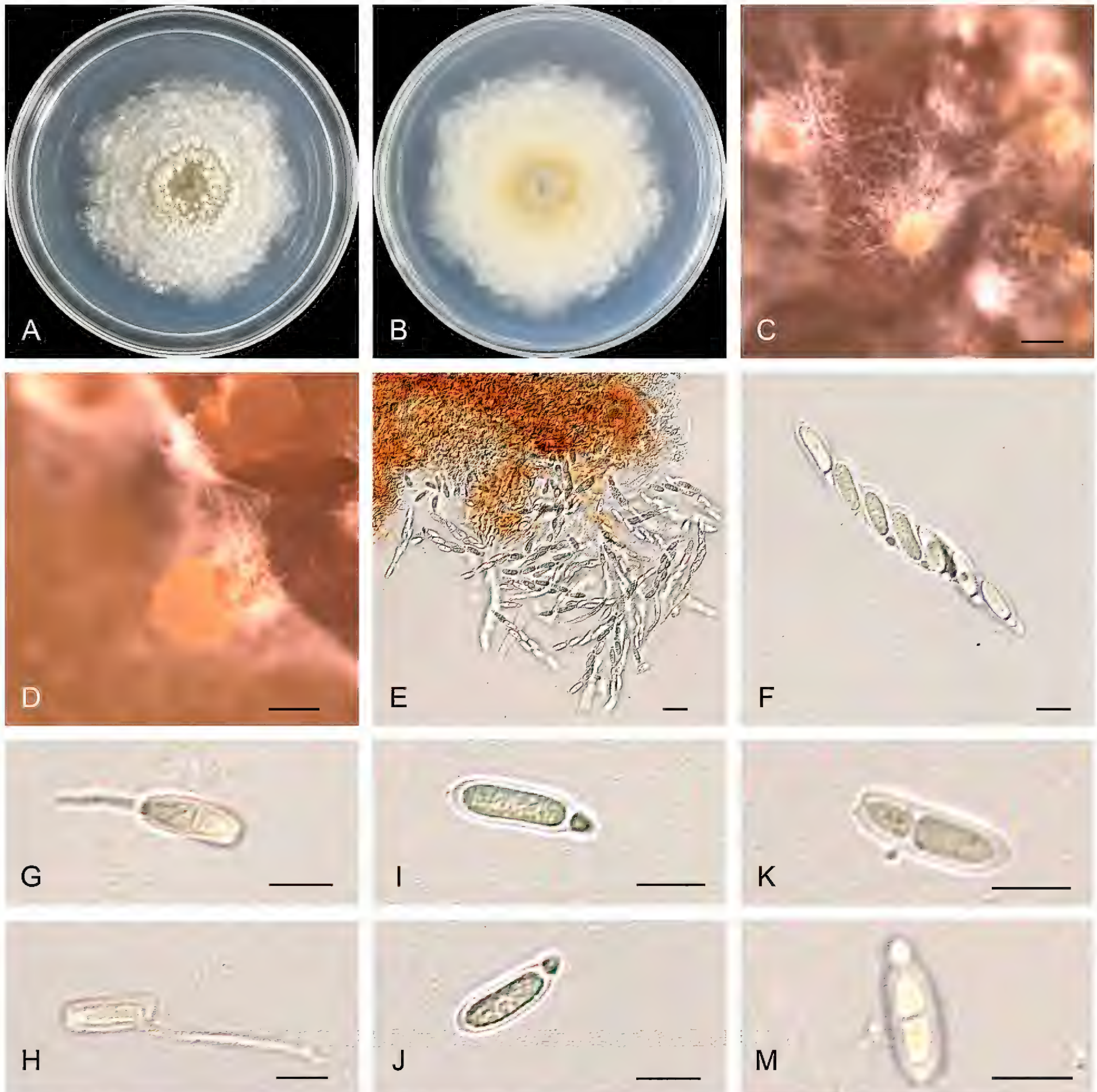

Figure 7. *Ternstroemiomyces zhaoqingensis* (CGMCC 3.29460). **A, B.** Inverse and reverse sides of colony after seven days on PDA; **C, D.** Ascomata forming on PDA; **E, F.** Asci; **G, H.** The germinating ascospore; **I–M.** Ascospore. Scale bars: 200 μm (**C, D**); 20 μm (**E**); 10 μm (**F–M**).

which precluded direct comparison of microscopic structures with *Te. ternstroemiae* and *Te. machili*. A synopsis of morphological and cultural characteristics is presented in Table 3. Nevertheless, the three species showed differences in their cultural characteristics on PDA. Although colony growth rate is generally regarded as a supplementary character, *Te. zhaoqingensis* (8.7–9.1 mm/d) exhibited a noticeably faster growth rate than *Te. ternstroemiae* (4.5–4.8 mm/d) and *Te. machili* (2.8–3.3 mm/d) when cultured under identical conditions. In addition, differences were observed in colony morphology: colonies of *Te. zhaoqingensis* were dense and cottony, white with a yellowish-white center. In contrast, colonies of *Te. machili* appeared gray-white with relatively sparse mycelia, while those of *Te. ternstroemiae* showed white to grayish aerial mycelium.

Table 3. Synopsis of morphological and cultural characteristics of *Te. zhaoqingensis* and *Te.cinnamomi* compared with closely related species.

Species	Conidia (Asexual) (μm)	Ascospores (Sexual) (μm)	Colony characteristics (on PDA)	Growth rate (mm/d)	Reference
Te. cinnamomi	10.5–14.5 × 5–7.6	Not observed	white with moderate mycelia	8.4–9.1	This study
Te. zhaoqingensis	Not observed	11.5–18.1 × 4.8–6.8	yellowish-white with dense mycelia	8.7–9.1	This study
Te. machili	11–18.5 × 8.2–10.5	Not observed	gray-white with little mycelia	2.8–3.3	Zhang et al. (2025)
Te. ternstroemiae	18–22(–25) × 8.7–10	Not observed	gray-white with moderate mycelia	4.5–4.8	Zhang et al. (2025)

Taken together, these macroscopic characteristics provide supportive, though not definitive, phenotypic evidence that is consistent with the phylogenetic separation of *Te. zhaoqingensis*. The new isolates are therefore described here as *Ternstroemiomyces zhaoqingensis* sp. nov., based on the combined evidence from cultural characteristics and phylogenetic analyses.

Discussion

The taxonomic system of the order Diaporthales has undergone a profound paradigm shift: its early framework was exclusively based on the morphological characteristics of the teleomorph (Barr 1978), yet the limitations of this approach prompted a gradual transition toward a more integrative paradigm. Early morphology-based systems were often insufficient due to extensive morphological convergence and plasticity among taxa. This transformation has been driven by molecular phylogenetics, which, through the incorporation of multi-gene sequence data such as ITS, LSU, *rpb2*, and *tef1*, together with the integration of teleomorph and anamorph characteristics with molecular evidence, has successfully resolved numerous long-standing taxonomic ambiguities (Castlebury et al. 2002; Hyde et al. 2020). As demonstrated in recent taxonomic work, this integrated approach has successfully established a well-resolved classification system comprising 35 families (Zhang et al. 2025). The present study follows this integrative taxonomic framework. This study reports the first isolation and identification of three endophytic fungi belonging to the order Diaporthales from healthy leaves of *Cinnamomum cassia*. They are described as *Gnomoniopsis luodingensis* sp. nov., *Ternstroemiomyces cinnamomi* sp. nov., and *Ternstroemiomyces zhaoqingensis* sp. nov. Their taxonomic placement was inferred based on a combination of morphological observations and multilocus phylogenetic analyses (ITS, LSU, *tef1*), although some limitations in character comparability and locus coverage should be acknowledged.

In the phylogenetic analysis of *Gnomoniopsis*, LSU sequences were unavailable for three taxa (*G. hainanensis*, *G. fujianensis*, and *G. fagacearum*), and the *tef1* sequence of the sister lineage (*G. hainanensis*) was relatively short, preventing reliable base-by-base comparisons. Notably, single-locus analysis based on ITS placed *G. luodingensis* on a long branch, appearing as sister to the clade containing *G. hainanensis*, *G. fujianensis*, and *G. fagacearum*, but did not clearly resolve its specific relationship with *G. hainanensis*. We considered the possibility of phylogenetic artifacts, such as long-branch attraction (LBA), which may result from rate heterogeneity or limited phylogenetic signal in a single locus. In contrast, the concatenated multi-locus phylogeny provided improved resolution, recovering *G. luodingensis* as the sister species to *G. hainanensis* with strong support (BP: 92).

These results indicate that the multi-locus dataset contributed to resolving the topological uncertainty observed in the single-locus analysis and provided additional evidence for the delimitation of the new species. Morphologically, *G. luodingensis* conforms well to the generic description of *Gnomoniopsis* (Walker et al. 2010). It is characterized by globose conidiomata that are buried in or attached to mycelia, and conidia that are oblong to ellipsoid, smooth, aseptate, and guttulate.

According to previous studies, species of *Gnomoniopsis* are significant pathogens of agricultural and forestry crops, including trees, flowers, and fruit, often causing severe plant damage that leads to substantial economic losses (Miller and Lewis Ivey 2025). Species of *Gnomoniopsis* have been primarily reported on hosts within the Rosaceae, Fagaceae, and Onagraceae families (Guan et al. 2024; Li et al. 2025b). Recent research has extended this range to several other families, as documented by the discoveries of *G. annonae* on *Annona montana* (Annonaceae), *G. euryae* on *Eurya nitida* (Theaceae), *G. juglandis* on *Juglans regia* (Juglandaceae), *G. lanceolata* on *Phoebe lanceolata* (Lauraceae), and *G. melastomatis* on *Melastoma candidum* (Melastomataceae) (Zhang et al. 2025). These findings indicate that the host range of Gnomoniopsis is broader than previously assumed. Importantly, our study further expands the known host spectrum of *Gnomoniopsis* by reporting its presence on *Cinnamomum cassia* (Lauraceae). This finding explicitly extends the host range of the genus to include the laurel family, corroborating and adding a new host record to the earlier report of *G. lanceolata* on another lauraceous plant, *Phoebe lanceolata* (Zhang et al. 2025).

According to the latest classification by Zhang et al. (2025), the newly described family Ternstroemiomycetaceae is closely allied with Erythrogloeaceae, together forming a separate clade in a larger phylogenetic grouping (a relationship also supported by our Fig. 4). A similar issue regarding data availability was observed in the phylogenetic analysis of *Ternstroemiomyces*. The *tef1* sequences for the sister taxa, *Te. machili* and *Te. ternstroemiae*, were relatively short, preventing reliable base-by-base comparisons and limiting resolution within this subclade. We considered the possibility that the distinct positions of the new species could result from long-branch attraction (LBA) due to these data limitations. Nevertheless, both single-locus (ITS) and concatenated multi-locus phylogenies consistently recovered *Te. cinnamomi* and *Te. zhaoqingensis* as separate lineages. In the multi-locus analysis, they formed well-supported clades (BP/PP = 99/1), each sisters to *Te. machili* and *Te. ternstroemiae*, respectively. This concordance across different datasets, despite partial sequence incompleteness in sister taxa, provides additional evidence that the new species represent genetically distinct lineages rather than artifacts of phylogenetic reconstruction.

Morphologically, the sexual morph of *Ternstroemiomyces cinnamomi* is distinct from other families in Diaporthales. It differs from Harknessiaceae and Schizoparmaceae primarily in having consistently 1-septate ascospores, whereas ascospores in these two families are typically aseptate (Senanayake et al. 2017). In addition, the sub-lageniform ascospores with apically attenuated ends further distinguish *Te. cinnamomi* from the predominantly ellipsoidal ascospores observed in Schizoparmaceae. With respect to Erythrogloeaceae (Senanayake et al. 2017), the sexual morph characters are poorly defined or remain undocumented for most representative taxa, rendering a reliable morphological comparison currently unfeasible. Nevertheless, multigene phylogenetic analyses place

Te. cinnamomi unambiguously within Ternstroemiomycetaceae, supporting its taxonomic independence from these morphologically comparable families.

During an investigation of endophytic fungi associated with *C. cassia*, three novel taxa were identified from healthy leaf tissues. These results highlight the still-underexplored diversity of endophytic Diaporthales associated with Lauraceae. Ecologically, the recovery of these taxa as endophytes suggests that they may be involved in host–fungus interactions; however, their specific ecological roles remain unclear. Endophytic fungi are known to exhibit a broad spectrum of lifestyles, ranging from mutualism to latent pathogenicity, and may influence host physiology under certain conditions. Previous studies have demonstrated that some functional endophytes can enhance host stress tolerance and secondary metabolite accumulation through molecular regulation. For example, endophytic fungi associated with *Fagopyrum tataricum* have been shown to upregulate key biosynthetic genes (e.g., *C4H*, *CHS*, and *CHI*) and photosynthetic pathways, thereby improving flavonoid production and drought resistance (Jia et al. 2025). However, such ecological roles remain speculative in the absence of experimental or functional evidence. This study underscores the unique resources of endophytic fungi in economically important trees. Future research integrating functional assays, pathogenicity tests, and omics-based approaches will be necessary to clarify the ecological roles and applied potential of these taxa.

Additional information

Conflict of interest

The authors have declared that no competing interests exist.

Ethical statement

No ethical statement was reported.

Use of AI

No use of AI was reported.

Funding

This work was supported by the Central Government Guides Local Science and Technology Development Fund (Grant No. ZY22096003); and the Guangxi Natural Science Foundation (Grant Nos. 2025GXNSFAA069563, 2019GXNSFDA245017); the Guangxi Major Science and Technology Project (Grant No. AA22096029).

Author contributions

Zheng-Hu Guo and Ya-Qin Zhou contributed equally to this work. Zheng-Hu Guo, Ya-Qin Zhou, and Jie Wang conceived and designed the experiments. Ya-Qin Zhou, Li-Ying Yu, and Shou-Jie Qin performed the experiments and collected the data. Jia-Xin Liu and Yu Chen conducted the formal data analysis and visualization. Rong-Shao Huang provided materials. The manuscript was drafted by Zheng-Hu Guo and Ya-Qin Zhou, and critically revised by Xiao-Ming Tan. Xiao-Ming Tan supervised the entire project and acquired funding. All authors reviewed and approved the final manuscript.

Author ORCIDs

Zheng-Hu Guo https://orcid.org/0009-0008-7195-8458

Data availability

All of the data that support the findings of this study are available in the main text.

References

Bai Y, Lin L, Pan M, Fan X (2023) Studies of *Diaporthe* (Diaporthaceae, Diaporthales) species associated with plant cankers in Beijing, China, with three new species described. MycoKeys 98: 59–86. https://doi.org/10.3897/mycokeys.98.104156

Barr ME (1978) The Diaporthales in North America with emphasis on *Gnomonia* and its segregates. Mycologia Memoirs 7: 1–232.

Castlebury LA, Rossman AY, Jaklitsch WJ, Vasilyeva LN (2002) A preliminary overview of the Diaporthales based on large subunit nuclear ribosomal DNA sequences. Mycologia 94(6): 1017–1031. https://doi.org/10.1080/15572536.2003.11833157

Cheewangkoon R, Groenewald JZ, Summerell BA, Hyde KD, To-Anun C, Crous PW (2009) Myrtaceae, a cache of fungal biodiversity. Persoonia 23: 55–85. https://doi.org/10.3767/003158509X474752

Chen Q, Bakhshi M, Balci Y, Broders KD, Cheewangkoon R, Chen SF, Fan XL, Gramaje D, Halleen F, Horta Jung M, Jiang N, Jung T, Májek T, Marincowitz S, Milenković I, Mostert L, Nakashima C, Nurul Faziha I, Pan M, Raza M, Scanu B, Spies CFJ, Suhaizan L, Suzuki H, Tian CM, Tomšovský M, Úrbez-Torres JR, Wang W, Wingfield BD, Wingfield MJ, Yang Q, Yang X, Zare R, Zhao P, Groenewald JZ, Cai L, Crous PW (2022) Genera of phytopathogenic fungi: GOPHY 4. Studies in Mycology 101: 417–564. https://doi.org/10.3114/sim.2022.101.06

Cheng Y, Fu Y, Gu D, Huang Y, Lu Y, Liu Y, Li X, Yao X, Zhang X, Jian W, Liu P, Wu H, Li Y (2024) Seasonal variation in chemical composition and antioxidant and antibacterial activity of essential oil from *Cinnamomum cassia* leaves. Plants 14(1): 81. https://doi.org/10.3390/plants14010081

Crous PW, Summerell BA, Alfenas AC, Edwards J, Pascoe IG, Porter IJ, Groenewald JZ (2012a) Genera of diaporthalean coelomycetes associated with leaf spots of tree hosts. Persoonia 28: 66–75. https://doi.org/10.3767/003158512X642030

Crous PW, Summerell BA, Shivas RG, Carnegie AJ, Groenewald JZ (2012b) A re-appraisal of *Harknessia* (Diaporthales), and the introduction of Harknessiaceae fam. nov. Persoonia 28: 49–65. https://doi.org/10.3767/003158512X639791

Crous PW, Summerell BA, Shivas RG, Burgess TI, Decock CA, Dreyer LL, Granke LL, Guest DI, Hardy GE, Hausbeck MK, Hüberli D, Jung T, Koukol O, Lennox CL, Liew EC, Lombard L, McTaggart AR, Pryke JS, Roets F, Saude C, Shuttleworth LA, Stukely MJ, Vánky K, Webster BJ, Windstam ST, Groenewald JZ (2012c) Fungal Planet description sheets: 107–127. Persoonia 28: 138–182. https://doi.org/10.3767/003158512X652633

Crous PW, Wingfield MJ, Guarro J, Cheewangkoon R, van der Bank M, Swart WJ, Stchigel AM, Cano-Lira JF, Roux J, Madrid H, Damm U, Wood AR, Shuttleworth LA, Hodges CS, Munster M, de Jesús Yáñez-Morales M, Zúñiga-Estrada L, Cruywagen EM, de Hoog GS, Silvera C, Najafzadeh J, Davison EM, Davison PJ, Barrett MD, Barrett RL, Manamgoda DS, Minnis AM, Kleczewski NM, Flory SL, Castlebury LA, Clay K, Hyde KD, Maússe-Sitoe SN, Chen S, Lechat C, Hairaud M, Lesage-Meessen L, Pawłowska J, Wilk M, Sliwińska-Wyrzychowska A, Mętrak M, Wrzosek M, Pavlic-Zupanc D, Maleme HM, Slippers B, Mac Cormack WP, Archuby DI, Grünwald NJ, Tellería MT, Dueñas M, Martín MP, Marincowitz S, de Beer ZW, Perez CA, Gené J, Marin-Felix Y, Groenewald JZ (2013) Fungal Planet description sheets: 154–213. Persoonia 31: 188–296. https://doi.org/10.3767/003158513X675925

Crous PW, Luangsa-Ard JJ, Wingfield MJ, Carnegie AJ, Hernández-Restrepo M, Lombard L, Roux J, Barreto RW, Baseia IG, Cano-Lira JF, Martín MP, Morozova OV, Stchigel AM, Summerell BA, Brandrud TE, Dima B, García D, Giraldo A, Guarro J, Gusmão LFP, Khamsuntorn P, Noordeloos ME, Nuankaew S, Pinruan U, Rodríguez-Andrade E, Souza-Motta CM, Thangavel R, van Iperen AL, Abreu VP, Accioly T, Alves JL, Andrade JP, Bahram M, Baral HO, Barbier E, Barnes CW, Bendiksen E, Bernard E, Bezerra JDP, Bezerra JL, Bizio E, Blair JE, Bulyonkova TM, Cabral TS, Caiafa MV, Cantillo T, Colmán AA, Conceição LB, Cruz S, Cunha AOB, Darveaux BA, da Silva AL, da Silva GA, da Silva GM, da Silva RMF, de Oliveira RJV, Oliveira RL, De Souza JT, Dueñas M, Evans HC, Epifani F, Felipe MTC, Fernández-López J, Ferreira BW, Figueiredo CN, Filippova NV, Flores JA, Gené J, Ghorbani G, Gibertoni TB, Glushakova AM, Healy R, Huhndorf SM, Iturrieta-González I, Javan-Nikkhah M, Juciano RF, Jurjević Ž, Kachalkin AV, Keochanpheng K, Krisai-Greilhuber I, Li YC, Lima AA, Machado AR, Madrid H, Magalhães OMC, Marbach PAS, Melanda GCS, Miller AN, Mongkolsamrit S, Nascimento RP, Oliveira TGL, Ordoñez ME, Orzes R, Palma MA, Pearce CJ, Pereira OL, Perrone G, Peterson SW, Pham THG, Piontelli E, Pordel A, Quijada L, Raja HA, Rosas de Paz E, Ryvarden L, Saitta A, Salcedo SS, Sandoval-Denis M, Santos TAB, Seifert KA, Silva BDB, Smith ME, Soares AM, Sommai S, Sousa JO, Suetrong S, Susca A, Tedersoo L, Telleria MT, Thanakitpipattana D, Valenzuela-Lopez N, Visagie CM, Zapata M, Groenewald JZ (2018) Fungal Planet description sheets: 785–867. Persoonia 41: 238–417. https://doi.org/10.3767/persoonia.2018.41.12

Crous PW, Wingfield MJ, Cheewangkoon R, Carnegie AJ, Burgess TI, Summerell BA, Edwards J, Taylor PWJ, Groenewald JZ (2019) Foliar pathogens of eucalypts. Studies in Mycology 94: 125–298. https://doi.org/10.1016/j.simyco.2019.08.001

Crous PW, Wingfield MJ, Chooi YH, Gilchrist CLM, Lacey E, Pitt JI, Roets F, Swart WJ, Cano-Lira JF, Valenzuela-Lopez N, Hubka V, Shivas RG, Stchigel AM, Holdom DG, Jurjević Ž, Kachalkin AV, Lebel T, Lock C, Martín MP, Tan YP, Tomashevskaya MA, Vitelli JS, Baseia IG, Bhatt VK, Brandrud TE, De Souza JT, Dima B, Lacey HJ, Lombard L, Johnston PR, Morte A, Papp V, Rodríguez A, Rodríguez-Andrade E, Semwal KC, Tegart L, Abad ZG, Akulov A, Alvarado P, Alves A, Andrade JP, Arenas F, Asenjo C, Ballarà J, Barrett MD, Berná LM, Berraf-Tebbal A, Bianchinotti MV, Bransgrove K, Burgess TI, Carmo FS, Chávez R, Čmoková A, Dearnaley JDW, Santiago ALCMA, Freitas-Neto JF, Denman S, Douglas B, Dovana F, Eichmeier A, Esteve-Raventós F, Farid A, Fedosova AG, Ferisin G, Ferreira RJ, Ferrer A, Figueiredo CN, Figueiredo YF, Reinoso-Fuenteal-ba CG, Garrido-Benavent I, Cañete-Gibas CF, Gil-Durán C, Glushakova AM, Gonçalves MFM, González M, Gorczak M, Gorton C, Guard FE, Guarnizo AL, Guarro J, Gutiérrez M, Hamal P, Hien LT, Hocking AD, Houbraken J, Hunter GC, Inácio CA, Jourdan M, Kapitonov VI, Kelly L, Khanh TN, Kisło K, Kiss L, Kiyashko A, Kolařík M, Kruse J, Kubátová A, Kučera V, Kučerová I, Kušan I, Lee HB, Levicán G, Lewis A, Liem NV, Liimatainen K, Lim HJ, Lyons MN, Maciá-Vicente JG, Magaña-Dueñas V, Mahiques R, Malysheva EF, Marbach PAS, Marinho P, Matočec N, McTaggart AR, Mešić A, Morin L, Muñoz-Mohedano JM, Navarro-Ródenas A, Nicolli CP, Oliveira RL, Otsing E, Ovrebo CL, Pankratov TA, Paños A, Paz-Conde A, Pérez-Sierra A, Phosri C, Pintos Á, Pošta A, Prencipe S, Rubio E, Saitta A, Sales LS, Sanhueza L, Shuttleworth LA, Smith J, Smith ME, Spadaro D, Spetik M, Sochor M, Sochorová Z, Sousa JO, Suwannasai N, Tedersoo L, Thanh HM, Thao LD, Tkalčec Z, Vaghefi N, Venzhik AS, Verbeken A, Vizzini A, Voyron S, Wainhouse M, Whalley AJS, Wrzosek M, Zapata M, Zeil-Rolfe I, Groenewald JZ (2020) Fungal Planet description sheets: 1042–1111. Persoonia 44(1): 301–459. https://doi.org/10.3767/persoonia.2020.44.11

Dobry E, Campbell M (2023) *Gnomoniopsis castaneae*: An emerging plant pathogen and global threat to chestnut systems. Plant Pathology 72(2): 218–231. https://doi.org/10.1111/ppa.13670

Fan XL, Bezerra JDP, Tian CM, Crous PW (2018) Families and genera of diaporthalean fungi associated with canker and dieback of tree hosts. Persoonia 40: 119–134. https://doi.org/10.3767/persoonia.2018.40.05

Gomes RR, Glienke C, Videira SI, Lombard L, Groenewald JZ, Crous PW (2013) *Diaporthe*: A genus of endophytic, saprobic and plant pathogenic fungi. Persoonia 31: 1–41. https://doi.org/10.3767/003158513X666844

Guan X, Mu T, Keyhani NO, Shang J, Mao Y, Yang J, Zheng M, Yang L, Pu H, Lin Y, Zhu M, Lv H, Heng Z, Liang H, Fan L, Ma X, Ma H, Qiu Z, Qiu J (2024) New species of Diaporthales (Ascomycota) from diseased leaves in Fujian Province, China. Journal of Fungi (Basel, Switzerland) 11(1): 8. https://doi.org/10.3390/jof11010008

Guo LD, Hyde KD, Liew ECY (2000) Identification of endophytic fungi from Livistona chinensis based on morphology and rDNA sequences. The New Phytologist 147(3): 617–630.

Huelsenbeck JP, Ronquist F (2001) MRBAYES: Bayesian inference of phylogeny trees. Bioinformatics (Oxford, England) 17(17): 754–755. https://doi.org/10.1093/bioinformatics/17.8.754

Hyde KD, Norphanphoun C, Maharachchikumbura SS, Bhat DJ, Jones E, Bundhun D, Chen YJ, Bao DF, Boonmee S, Calabon MS, Chaiwan N (2020) Refined families of Sordariomycetes. Mycosphere 11(1): 305–1059. https://doi.org/10.5943/mycosphere/11/1/7

Jaklitsch WM, Voglmayr H (2019) European species of *Dendrostoma* (Diaporthales). MycoKeys 59: 1–26. https://doi.org/10.3897/mycokeys.59.37966

Jia Y, Xie Q, Tao J, Chen Y, Qi Y, Zhu H, Bu T, Zhang X, Xiao Y, Chen Z, Li Q (2025) Endophytic fungi enhance drought tolerance in *Fagopyrum tataricum*: Insights into flavonoid biosynthesis and photosynthetic pathways. Agricultural Water Management 313: 109496. https://doi.org/10.1016/j.agwat.2025.109496

Jiang N, Fan XL, Crous PW, Tian CM (2019) Species of *Dendrostoma* (Erythrogloeaceae, Diaporthales) associated with chestnut and oak canker diseases in China. MycoKeys 48: 67–96. https://doi.org/10.3897/mycokeys.48.31715

Jiang N, Fan X, Tian C, Crous PW (2020a) Reevaluating Cryphonectriaceae and allied families in Diaporthales. Mycologia 112(2): 267–292. https://doi.org/10.1080/00275514.2019.1698925

Jiang N, Liang LY, Tian CM (2020b) *Gnomoniopsis chinensis* (Gnomoniaceae, Diaporthales), a new fungus causing canker of Chinese chestnut in Hebei Province, China. MycoKeys 67: 19–32. https://doi.org/10.3897/mycokeys.67.51133

Jiang N, Voglmayr H, Bian DR, Piao CG, Wang SK, Li Y (2021) Morphology and phylogeny of *Gnomoniopsis* (Gnomoniaceae, Diaporthales) from Fagaceae leaves in China. Journal of Fungi (Basel, Switzerland) 7(10): 792. https://doi.org/10.3390/jof7100792

Jiang L, Ma QX, Li AJ, Sun RZ, Tang GY, Huang XS, Pu H (2023) Bioactive secondary metabolites produced by fungi of the genus *Diaporthe* (*Phomopsis*): Structures, biological activities, and bio synthesis. Arabian Journal of Chemistry 16(9): 105062. https://doi.org/10.1016/j.arabjc.2023.105062

Jiang N, Qi X, Qi B, Cai F, Xue H, Li Y (2024) Two new species of *Dendrostoma* (Erythrogloeaceae, Diaporthales) associated with Castaneamollissima canker disease in China. MycoKeys 108: 337–349. https://doi.org/10.3897/mycokeys.108.128197

Katoh K, Standley DM (2013) MAFFT multiple sequence alignment software version 7: Improvements in performance and usability. Molecular Biology and Evolution 30(4): 772–780. https://doi.org/10.1093/molbev/mst010

Lee S, Groenewald JZ, Crous PW (2004) Phylogenetic reassessment of the coelomycete genus *Harknessia* and its teleomorph *Wuestneia* (Diaporthales), and the introduction of *Apoharknessia* gen. nov. Studies in Mycology 50: 235–252.

Letunic I, Bork P (2024) Interactive Tree of Life (iTOL) v6: Recent updates to the phylogenetic tree display and annotation tool. Nucleic Acids Research 52(W1): W78–W82. https://doi.org/10.1093/nar/gkae268

Li X, Xu X, Xiang S, Liu F, Wang F, Jiang X, Liu Y, Yang C (2025a) Morpho-phylogenetic evidence reveals two new species and two new host records of *Diaporthe* (Diaporthales, Diaporthaceae) from *Phellodendron chinense* in Sichuan, China. MycoKeys 123: 205–233. https://doi.org/10.3897/mycokeys.123.162866

Li Y, Li A, Jiang N (2025b) Identification of the nut rot pathogen affecting *Castanopsis carlesii* based on morphological and phylogenetic analyses. Forests 16(4): 627. https://doi.org/10.3390/f16040627

Liu YC, Linder-Basso D, Hillman BI, Kaneko S, Milgroom MG (2003) Evidence for interspecies transmission of viruses in natural populations of filamentous fungi in the genus *Cryphonectria*. Molecular Ecology 12(6): 1619–1628. https://doi.org/10.1046/j.1365-294x.2003.01847.x

Lv J, Zhou H, Dong L, Wang H, Yang L, Yu H, Wu P, Zhou L, Yang Q, Liang Y, Luo B (2024) Three new furanones from endophytic fungus *Hypoxylon vinosopulvinatum* DYR-1-7 from *Cinnamomum cassia* with their antifungal activity. Natural Product Research 38(18): 3165–3172. https://doi.org/10.1080/14786419.2023.2218530

Miller AC, Lewis Ivey ML (2025) The disease triangle of chestnut: A review of host, pathogen, and environmental interactions of chestnuts cultivated in the eastern United States. Plant Disease 109(2): 245–256. https://doi.org/10.1094/PDIS-11-23-2355-FE

Minh BQ, Schmidt HA, Chernomor O, Schrempf D, Woodhams MD, von Haeseler A, Lanfear R (2020) Corrigendum to: IQ-TREE 2: New models and efficient methods for phylogenetic inference in the genomic era. Molecular Biology and Evolution 37(8): 2461. https://doi.org/10.1093/molbev/msaa131

Pereira EC, Zabalgogeazcoa I, Arellano JB, Ugalde U, Aldana BRV (2023) *Diaporthe atlantica* enhances tomato drought tolerance by improving photosynthesis, nutrient uptake and enzymatic antioxidant response. Frontiers in Plant Science 14(1): 1–13. https://doi.org/10.3389/fpls.2023.1118698

Rehner S, Buckley E (2005) A *Beauveria* phylogeny inferred from nuclear ITS and EF1-α sequences: Evidence for cryptic diversification and links to *Cordyceps* teleomorphs. Mycologia 97(1): 84–98. https://doi.org/10.3852/mycologia.97.1.84

Samarakoon MC, Promputtha I, Liu JK (2021) *Dendrostoma covidicola* sp. nov. (Erythrogloeaceae, Diaporthales) on *Fagus sylvatica* from Sichuan Province, China. Phytotaxa 483(2): 85–94. https://doi.org/10.11646/phytotaxa.483.2.1

Saravanakumar K, Sriram B, Sathiyaseelan A, Hu XW, Mariadoss AVA, MubarakAli D, Wang MH (2021) Molecular identification, volatile metabolites profiling, and bioactivities of an indigenous endophytic fungus (*Diaporthe* sp.). Process Biochemistry (Barking, London, England) 102: 72–81. https://doi.org/10.1016/j.procbio.2020.12.002

Senanayake IC, Crous PW, Groenewald JZ, Maharachchikumbura SSN, Jeewon R, Phillips AJL, Bhat JD, Perera RH, Li QR, Li WJ, Tangthirasunun N, Norphanphoun C, Karunarathna SC, Camporesi E, Manawasighe IS, Al-Sadi AM, Hyde KD (2017) Families of Diaporthales based on morphological and phylogenetic evidence. Studies in Mycology 86: 217–296. https://doi.org/10.1016/j.simyco.2017.07.003

Sogonov MV, Castlebury LA, Rossman AY, White JF (2007) The type species of *Apiognomonia*, *A. veneta*, with its *Discula* anamorph is distinct from

A. errabunda. Mycological Research 111(6): 693–709. https://doi.org/10.1016/j.mycres.2007.03.013

Sogonov MV, Castlebury LA, Rossman AY, Mejía LC, White JF (2008) Leaf-inhabiting genera of the Gnomoniaceae, Diaporthales. Studies in Mycology 62: 1–77. https://doi.org/10.3114/sim.2008.62.01

Sun K, Zhang FM, Kang N, Gong JH, Zhang W, Chen Y, Dai CC (2019) Rice carbohydrate dynamics regulate endophytic colonization of *Diaporthe liquidambaris* in response to external nitrogen. Fungal Ecology 39(5): 213–224. https://doi.org/10.1016/j.funeco.2019.02.010

Tziros GT (2019) First report of nut rot caused by *Gnomoniopsis castaneae* on *Castanea sativa* in Greece. Journal of Plant Pathology 101: 211. https://doi.org/10.1007/s42161-018-0161-4

Van Niekerk JM, Groenewald JZ, Verkley GJ, Fourie PH, Wingfield MJ, Crous PW (2004) Systematic reappraisal of *Coniella* and *Pilidiella*, with specific reference to species occurring on *Eucalyptus* and *Vitis* in South Africa. Mycological Research 108(3): 283–303. https://doi.org/10.1017/s0953756204009268

Vilgalys R, Hester M (1990) Rapid genetic identification and mapping of enzymatically amplified ribosomal DNA from several *Cryptococcus* species. Journal of Bacteriology 172(8): 4238–4246. https://doi.org/10.1128/jb.172.8.4238-4246.1990

Vu D, Groenewald M, de Vries M, Gehrmann T, Stielow B, Eberhardt U, Al-Hatmi A, Groenewald JZ, Cardinali G, Houbraken J, Boekhout T, Crous PW, Robert V, Verkley GJM (2019) Large-scale generation and analysis of filamentous fungal DNA barcodes boosts coverage for kingdom fungi and reveals thresholds for fungal species and higher taxon delimitation. Studies in Mycology 92: 135–154. https://doi.org/10.1016/j.simyco.2018.05.001

Walker DM, Castlebury LA, Rossman AY, Sogonov MV, White JF (2010) Systematics of genus *Gnomoniopsis* (Gnomoniaceae, Diaporthales) based on a three gene phylogeny, host associations and morphology. Mycologia 102: 1479–1796. https://doi.org/10.3852/10-002

Wang SY, McKenzie EHC, Phillips AJL, Li Y, Wang Y (2022a) Taxonomy and multigene phylogeny of Diaporthales in Guizhou Province, China. Journal of Fungi (Basel, Switzerland) 8(12): 1301. https://doi.org/10.3390/jof8121301

Wang S, Zhang Z, Liu R, Liu S, Liu X, Zhang X (2022b) Morphological and phylogenetic analyses reveal four new species of *Gnomoniopsis* (Gnomoniaceae, Diaporthales) from China. Journal of Fungi (Basel, Switzerland) 8(8): 770. https://doi.org/10.3390/jof8080770

White TJ, Bruns T, Lee S, Taylor J (1990) Amplification and direct sequencing of fungal ribosomal RNA genes for phylogenetics. PCR Protocols, A Guide to Methods and Application (1): 315–322. https://doi.org/10.1016/b978-0-12-372180-8.50042-1

Winter G (1886) Fungi Australienses. Revue Mycologique 8: 207–213.

Xavier KV, Kc AN, Crous PW, Groenewald JZ, Vallad GE (2019) *Dwiroopa punicae* sp. nov. (Dwiroopaceae fam. nov., Diaporthales), associated with leaf spot and fruit rot of pomegranate (*Punica granatum*). Fungal Systematics and Evolution 4: 33–41. https://doi.org/10.3114/fuse.2019.04.04

Xiang CY, Gao F, Jakovlić I, Lei HP, Hu Y, Zhang H, Zou H, Wang GT, Zhang D (2023) Using PhyloSuite for molecular phylogeny and tree-based analyses. iMeta 2(1): e87. https://doi.org/10.1002/imt2.87

Xu TC, Lu YH, Wang JF, Song ZQ, Hou YG, Liu SS, Liu CS, Wu SH (2021) Bioactive secondary metabolites of the genus *Diaporthe* and anamorph *Phomopsis* from terrestrial

and marine habitats and endophytes: 2010–2019. Microorganisms 9(2): 217. https://doi.org/10.3390/microorganisms9020217

Zhang C, Fan L, Fan S, Wang J, Luo T, Tang Y, Chen Z, Yu L (2019) *Cinnamomum cassia* Presl: A review of its traditional uses, phytochemistry, pharmacology and toxicology. Molecules (Basel, Switzerland) 24(19): 3473. https://doi.org/10.3390/molecules24193473

Zhang ZX, Shang YX, Liu QY, Li DH, Yin CZ, Liu XY, Tao MF, Jiang Y, Wang YX, Zhang MY, Dong ZX, Yun JX, Xia JW, Wang S, Li Z, Luo ZL, Liu XY, Zhang XG (2025) Deciphering the evolutionary and taxonomic complexity of Diaporthales (Sordariomycetes, Ascomycota) through integrated phylogenomic and divergence time estimation. Fungal Diversity 132: 1–125. https://doi.org/10.1007/s13225-025-00551-4

Zhao L, Zhang L, Ding Y, Li M, Zhang Y (2025) *Diaporthe* species (Sordariomycetes, Diaporthales) causing walnut blight and dieback in China. MycoKeys 122: 197–221. https://doi.org/10.3897/mycokeys.122.158807

Zhou YQ, Yao SC, Wang J, Xie XY, Tan XM, Huang RS, Yang XF, Tan Y, Yu LY, Fu P (2022) Cultivable endophytic fungal community associated with the karst endemic plant *Nervilia fordii* and their antimicrobial activity. Frontiers in Microbiology 13: 1063897. https://doi.org/10.3389/fmicb.2022.1063897

Zhu H, Pan M, Bonthond G, Tian CM, Fan XL (2019) Diaporthalean fungi associated with canker and dieback of trees from Mount Dongling in Beijing, China. MycoKeys 59: 67–94. https://doi.org/10.3897/mycokeys.59.38055